Development 126, 3119-3130 (1999)
Printed in Great Britain © The Company of Biologists Limited 1999
DEV3013

The role of *tolloid/mini fin* in dorsoventral pattern formation of the zebrafish embryo

Stephanie A. Connors[1], Jamie Trout[1], Marc Ekker[2] and Mary C. Mullins[1,*]

[1]University of Pennsylvania School of Medicine, Department of Cell and Developmental Biology, 1211 BRBII, 421 Curie Blvd., Philadelphia, PA 19104-6058, USA
[2]University of Ottawa, Loeb Institute for Medical Research, 725 Parkdale Ave., Ottawa, Ontario, Canada
*Author for correspondence (e-mail: mullins@mail.med.upenn.edu)

Accepted 28 April; published on WWW 21 June 1999

SUMMARY

A highly conserved TGF-β signaling pathway is involved in the establishment of the dorsoventral axis of the vertebrate embryo. Specifically, Bone Morphogenetic Proteins (Bmps) pattern ventral tissues of the embryo while inhibitors of Bmps, such as Chordin, Noggin and Follistatin, are implicated in dorsal mesodermal and neural development. We investigated the role of Tolloid, a metalloprotease that can cleave Chordin and increase Bmp activity, in patterning the dorsoventral axis of the zebrafish embryo. Injection of *tolloid* mRNA into six dorsalized mutants rescued only one of these mutants, *mini fin*. Through chromosomal mapping, linkage and cDNA sequence analysis of several *mini fin* alleles, we demonstrate that *mini fin* encodes the *tolloid* gene. Characterization of the *mini fin* mutant phenotype reveals that Mini fin/Tolloid activity is required for patterning ventral tissues of the tail: the ventral fin, and the ventroposterior somites and vasculature. Gene expression studies show that *mfn* mutants exhibit reduced expression of ventrally restricted markers at the end of gastrulation, suggesting that the loss of ventral tail tissues is caused by a dorsalization occurring at the end of gastrulation. Based on the *mini fin* mutant phenotype and the expression of *tolloid*, we propose that Mini fin/Tolloid modifes the Bmp activity gradient at the end of gastrulation, when the ventralmost marginal cells of the embryo are in close proximity to the dorsal Chordin-expressing cells. At this time, unimpeded Chordin may diffuse to the most ventral marginal regions and inhibit high Bmp activity levels. In the presence of Mini fin/Tolloid, however, Chordin activity would be negatively modulated through proteolytic cleavage, thereby increasing Bmp signaling activity. This extracellular mechanism is amplified by an autoregulatory loop for *bmp* gene expression.

Key words: *tolloid*, Metalloprotease, Pattern formation, Tail, Tail bud, BMP, *chordin*, Dorsoventral

INTRODUCTION

Bone morphogenetic proteins (Bmps) and their signaling pathways are essential in the development of numerous tissues in vertebrates (reviewed in Hogan, 1996). One of the earliest developmental processes involving Bmp signaling is the establishment of the dorsoventral axis of the embryo. Overexpression experiments in the frog and fish implicate a Bmp signaling pathway in ventral cell fate specification (reviewed in Mullins, 1999; Thomsen, 1997). Mutants of *bmp2b* in the zebrafish (*swirl* mutants) demonstrate a requirement for Bmp2b in the specification of nearly all ventral cell fates (Kishimoto et al., 1997; Nguyen et al., 1998b). Repression of Bmp signaling is necessary for dorsal mesodermal and neural development and is mediated through the action of Bmp antagonists, molecules secreted from dorsal tissue that can bind and prevent Bmp ligands from activating their receptors (reviewed in Graff, 1997; Thomsen, 1997). Zebrafish mutants of *chordin* (*chordino* mutants; Fisher et al., 1997; Schulte-Merker et al., 1997), one of the Bmp antagonists, exhibit a moderate ventralized phenotype, consistent with models of *chordin (chd)* function.

Ectopic expression and loss-of-function studies suggest that cell types derived from different dorsoventral regions of the gastrula are specified by a gradient of Bmp activity, with high levels specifying ventral and low levels lateral cell fates (Dosch et al., 1997; Jones and Smith, 1998; Knecht and Harland, 1997; Neave et al., 1997; Nguyen et al., 1998b; Wilson et al., 1997). The Bmp activity gradient is not reflected in gene expression levels of *Bmp2* or *Bmp4*, since these genes are expressed uniformly in ventral regions or throughout the embryo (Chin et al., 1997; Nikaido et al., 1997, reviewed in Thomsen, 1997). The gradient of Bmp activity is thought to be generated by the diffusion of the Bmp antagonists, Chd, Noggin and Follistatin, from the dorsal organizer of the embryo towards ventral regions (Dosch et al., 1997; Jones and Smith, 1998; Knecht and Harland, 1997; Wilson et al., 1997). The presumptive gradients of Bmp antagonists would thus establish a gradient of Bmp

activity in an opposite direction to that of the Bmp antagonists. In dorsal regions there would be little or no Bmp activity, in lateral regions low activity, and in ventral regions the highest activity.

A conserved TGF-β signaling pathway establishes the dorsoventral axis of the *Drosophila* embryo (although designation of the axes is inverted between vertebrates and invertebrates; reviewed in De Robertis and Sasai, 1996; Mullins, 1998). In the fly, the *decapentaplegic (dpp)* and *short gastrulation (sog)* genes are orthologues to *bmp2/4* and *chd*, respectively. *dpp* specifies dorsal cell fates, while *sog*, expressed in ventral regions, diffuses dorsally and can repress *dpp* signaling. A further modulator of Dpp activity is the astacin family metalloprotease, Tolloid (Tld). Mutants of *tld* display phenotypes similar to moderate or weak *dpp* alleles (Ferguson and Anderson, 1992b). Increasing the level of *dpp* can suppress *tld* loss-of-function defects, suggesting that Tld acts to enhance Dpp activity (Ferguson and Anderson, 1992a,b).

Genes related to *Drosophila tld* have been isolated in zebrafish (*tld*, Blader et al., 1997), *Xenopus* (Xolloid, Goodman et al., 1998; Piccolo et al., 1997, and Xtld, Lin et al., 1997; Maéno et al., 1993), mouse (*mTld*/Bmp1, Fukagawa et al., 1994; Takahara et al., 1994, and mTll, Takahara et al., 1996), and human (mTld, Takahara et al., 1994). Overexpression of *Xolloid*/*tld* in frog and fish embryos causes a moderate ventralization of the embryo (Blader et al., 1997; Goodman et al., 1998; Piccolo et al., 1997), a phenotype resembling that of *chd* mutants in the zebrafish (Fisher et al., 1997; Hammerschmidt et al., 1996a). In epistasis tests, *Xolloid*/*tld* overexpression blocks a dorsalization induced by *chd*, but did not affect a dorsalization caused by *noggin* or *follistatin* (Blader et al., 1997; Marqués et al., 1997; Piccolo et al., 1997). These results suggest that *Xolloid*/*tld* acts upstream of *chd* to specifically inhibit its activity. Biochemical evidence in the fly, frog and fish demonstrates that Tld can proteolytically cleave Chd/Sog protein (Blader et al., 1997; Marqués et al., 1997; Piccolo et al., 1997). Additional data indicate that the released Bmp ligands can bind and activate their receptors (Piccolo et al., 1997).

In the fly, Tld plays a fundamental role in modifying the activity of Sog to generate a Bmp signaling gradient while, in the vertebrate embryo, the role played by Tld in dorsoventral patterning has not been established. Null mutants of the mouse *Bmp1*/*mTld* gene display defects in ventral body wall closure, likely due to improper Procollagen processing in the amnion (Suzuki et al., 1996). No abnormality in dorsoventral axis formation was found in these mutants; however, the *mTll* gene may play a role in this process in the mouse.

Here, we report on the genetic analysis of *tolloid* function in dorsoventral patterning of the zebrafish embryo. Overexpression of *tld* mRNA in embryos of six different zebrafish dorsalized mutants rescued the phenotype of only one of these mutants, *mini fin (mfn)*. Linkage analysis, molecular cloning and DNA sequence analysis of the *tld* gene from several mutant *mfn* alleles, demonstrate that *mfn* is a mutation in the *tld* gene. We found that *mfn* is required to establish the most ventral cell types of the tail: the ventral fin, somites and vasculature. The loss of Mini fin/Tolloid activity is first manifested by a reduction in ventrally restricted gene expression at the end of gastrulation. Furthermore, some *mfn* mutants exhibit an aberrant expansion of *chd* gene expression. We propose that *mfn/tld* gene activity is required at the end of gastrulation and within the tail bud, when the dorsal and ventralmost marginal cells of the embryo lie in close proximity and Chd may diffuse to the ventralmost vegetal regions. Tld/Mfn would act to inhibit Chd function at these stages, thus generating high Bmp activity levels in ventral vegetal regions of the embryo, which then specify ventral tail cell fates.

MATERIALS AND METHODS

In situ hybridizations and phenotypic analysis

In situ hybridizations were performed essentially as described by Schulte-Merker et al. (1992). The following probes were used: *bmp4* (Chin et al., 1997), *dlx3* (Akimenko et al., 1994), *eve1*(Joly et al., 1993), *flk1* (Thompson et al., 1998), *msxB* (Akimenko et al., 1995), *msxD* (Akimenko et al., 1995), *myoD* (Weinberg et al., 1996), *tld* (Blader et al., 1997) and *chd* (Miller-Bertoglio et al., 1997). For double in situ hybridization, embryos were incubated with both fluorescein- and digoxigenin-labeled antisense probes. The fluorescein-labeled probe was detected with anti-fluorescein antibodies and visualized with 5-bromo-6-chloro-3-indolyl phosphate and tetrazolium red. After antibody removal (0.1 M glycine, 0.1% Tween-20), embryos were incubated with anti-digoxigenin antibodies and processed as described above. Embryos were scanned with a Progres 3012 digital camera (Kontron Elektroniks) and the images processed with Adobe software.

mfn mutants were identified by their mutant phenotype at bud and later stages, or at bud and earlier stages by 25% percent of the embryos exhibiting a different staining pattern. When less than 25% showed an altered pattern, embryos were genotyped by PCR using a restriction fragment length polymorphism (RFLP) created by the mutation. In these cases, pictures were taken to document the in situ expression in individual embryos, then embryonic DNA was made as described below. PCR was performed using primers flanking the mutation (tm124a allele: S12 TGTGTCAAGCATAAAGACTGG, S13 TCTTCTCAATGAAAGTCACGC), the PCR product was cut with *Msp*I, and run on a 2% agarose gel. The mfn^{tm124a} mutation causes the loss of an *Msp*I restriction site.

Mutant embryos from different *mfn* alleles were placed into categories (A-E) at 2 days of development, when the ventral tail fin is well defined and variations in phenotype are the most pronounced.

mRNA injections

Synthetic *tld* mRNA was made from pCS2:Ztld-3′MT (Blader et al., 1997) and injected into the yolk of 1- to 4-cell-stage embryos as described in Westerfield (1995). Mutants of the following alleles were injected: $swirl^{dta72}$, $somitabun^{dtc24}$, $snailhouse^{ty68a}$, $piggytail^{ty40a}$ and $lost\text{-}a\text{-}fin^{tm110b}$ (all described in Mullins et al., 1996). Embryos from crosses between transheterozygous adult *mfn* fish ($mfn^{ty130a}/mfn^{tf215a}$) were injected, so that all progeny were mutant and could not be mistaken for wild-type siblings. A two-fold range of *tld* mRNA (80-160 pg) was injected.

Linkage and chromosomal mapping

Crosses between Tübingen (TÜ) strain fish carrying either the mfn^{tm124a}, mfn^{tb241c} or the mfn^{ty130a} mutation and polymorphic WIK or AB strain fish were used to generate map crosses. The *tm124a* allele was originally reported to be an allele of the *piggytail* gene (Mullins et al., 1996). Additional complementation analyses revealed that *tm124a* is an allele of the *mfn* gene. The mapping procedure and the WIK line are described in Rauch et al. (1997) and Knapik et al. (1996). Pools of about 25 F_2 *mfn* mutant embryos and wild-type

siblings were collected separately and stored in methanol at –20°C. We found that embryos stored in methanol yielded higher amounts of genomic DNA. Embryonic DNA and PCR was performed as described by Gates et al. (1999), with the following PCR conditions: 94°C for 1 minute, 5 cycles of 94°C for 30 seconds, 54°C for 2 minutes and 73°C for 1 minute followed by 35 cycles of 94°C for 30 seconds, 55°C for 30 seconds and 73°C for 1 minute. Linkage was found to markers on LG1: Z5508, 15 recombinants/156 meioses and Z1705 (see text) in a *mfn*^{tm124a} map cross; Z1463, 1 recombinant/86 meioses in a *mfn*^{tb241c} map cross.

To estimate the map position of the *tld* gene, PCR was carried out on 94 zebrafish/mouse somatic cell hybrid (Ekker et al., 1996) and 93 radiation hybrid cell lines (Hukriede et al., in preparation). The following oligonucleotides were used: GCATGGACAGTTTG-GCTGC and CGCTGACATAAACAATGGGC, within the 3′ untranslated region (UTR; GenBank accession #AF027596). PCR conditions were as previously described (Chevrette et al., 1997).

Single F_2 mutant and wild-type embryos from a *mfn*^{ty130a} mapping cross line were tested for segregation of the *mfn* mutation to an RFLP in the *tld* 3′UTR. The 3′UTR was amplified by PCR using primers Tld3′a, TTGAGAGACTGAAGACAGGG and Tld3′b, CAGAAAG-TCAGTCAACAGCG, and the product cut with *Msp*I.

Cloning of *mfn* alleles

About 50 mutant embryos were collected at 24 hours postfertilization (hpf) from crosses between heterozygotes of five *mfn* alleles (*ty130a, tm124a, tf215a, tn217b*, tb241c; Mullins et al., 1996). Control wild-type embryos from the TÜ strain (the strain in which the mutations were induced) were also collected. Total RNA was extracted with TRIzol Reagent (Gibco/BRL) according to the manufacturer's instructions. First-strand cDNA was synthesized from total RNA with the Superscript Preamplification System for First Strand Synthesis (Life Technologies). Two to three independent PCR reactions were performed using the primer pairs Tld5′a/Tld5′b, Tld1/Tld2 and Tld3/Tld4 on wild-type and mutant embryo cDNA. The PCR was performed as follows: 94°C for 3 minutes; 40 cycles of 57°C for 1 minute, 70°C for 3 minutes, 94°C for 1 minute; 57°C for 1 minute and 70°C for 20 minutes.

Primers used:
Tld5′a AGGGAAATGGGCACGTTTGG
Tld5′b AGCAGCAGATATAAGGAACCC
Tld1ACACACATCTGGAGGTCTAGG
Tld2ACACACACTCCTTAGATGGG
Tld3AAGTTCTGGTCTCTACAGACAG
Tld4TCAGAGAGCGCAAGACACC

PCR products were subcloned using the TA-PCR cloning kit (Invitrogen) or the pGEM-T Easy Vector System (Promega) according to the manufacturer's instructions. Clones from independent PCR reactions were sequenced using primers spaced the length of the gene. Sequences were analyzed using MacMolly software.

RESULTS

Overexpression of *tolloid* rescues *mini fin* mutant embryos

Our previous rescue results using overexpression of *bmp* ligand genes (Nguyen et al., 1998b) implicate two genes with dorsalized mutant phenotypes, *somitabun* and *snailhouse*, to act within a Bmp signaling pathway to establish ventral cell fates. Tld acts upstream of the Bmp ligands to cleave Chd and release Bmps. To examine whether *snailhouse* and *somitabun* act upstream or downstream of *tld*, we injected wild-type *tld* mRNA into 1- to 4-cell-stage mutant embryos and assayed for rescue of the mutant phenotype at 24-30 hpf. Overexpression of *tld* could not rescue *somitabun* or *snailhouse* mutant embryos (Table 1), suggesting that these genes act downstream of, or parallel to, *tld* in a Bmp signaling pathway. As expected, *tld* overexpression did not rescue *swirl/bmp2b* mutants (Table 1), since *swirl/bmp2b* is predicted to function downstream of *tld*.

We investigated whether three additional dorsalized mutants, *piggytail*, *lost-a-fin* and *mfn* (Mullins et al., 1996), could be rescued by overexpression of *tld* mRNA. We observed no rescue of *piggytail* or *lost-a-fin* mutant embryos (Table 1), indicating that these two genes do not act upstream of, or as, a *tld* metalloprotease. In contrast, *tld* overexpression rescued a majority of *mfn* mutant embryos to a wild-type or slightly ventralized phenotype (Table 1; Fig. 1), suggesting that the *mfn* gene functions upstream of, or encodes, a *tld* metalloprotease.

mini fin and *tolloid* are chromosomally linked

To determine if *mfn* could correspond to the *tld* gene, we examined the chromosomal locations of *mfn* and *tld*. We mapped the *mfn* mutation to a chromosomal position using simple sequence length polymorphic (SSLP) markers located

Table 1. Injection of *tolloid* mRNA into dorsalized mutant embryos

	tolloid mRNA-injected embryos[a]								Uninjected embryos[a]						
gene	% rescued mutants	% WT/ vent.[b]	% C1	% C2	% C3	% C4	% C5	Total no.	% WT	% C1	% C2	% C3	% C4	% C5	Total no.
somitabun[c]	0	0	0	0	0	19	81	306	0	0	0	0	31	69	117
snailhouse[d]	0	0	0	0	0	2.9	97	70	0	0	0	0	21	79	78
swirl	0	56	19[e]	0	0	0	25	230	79	1.0	0	0	0	20	100
piggytail[f]	0	25	19	29	27	0	0	186	40	32	12	16	0	0	162
lost-a-fin	0	74	0	26	0	0	0	156	70	0	30	0	0	0	50
mini fin[g]	85	85	15	0	0	0	0	417	0	95	5	0	0	0	191
wildtype	NA	100[h]	0	0	0	0	0	166	100	0	0	0	0	0	121

[a]Mutant phenotypes were scored from class 1 to class 5 (C1-C5) according to Mullins et al. (1996) and are displayed as percentages.
[b]% WT/vent. refers to the percentage of embryos with a wildtype or ventralized phenotype.
[c]Dominant maternal mutation, thus 100% of embryos are mutant.
[d]Homozygous fish were mated to each other, thus 100% of embryos are mutant.
[e]In this experiment, we did not distinguish between weakly dorsalized and weakly ventralized embryos, the phenotypes of which can be similar. Hence, it is likely that this percentage includes embryos that are weakly ventralized.
[f]Dominant maternal-zygotic mutation exhibiting C1 to C3 phenotypes (Mullins et al., 1996).
[g]Transheterozygous (*mfn*^{ty130a}/*mfn*^{tf215a}) fish were mated to each other, thus 100% of embryos are mutant.
[h]92% of these embryos were visibly ventralized.

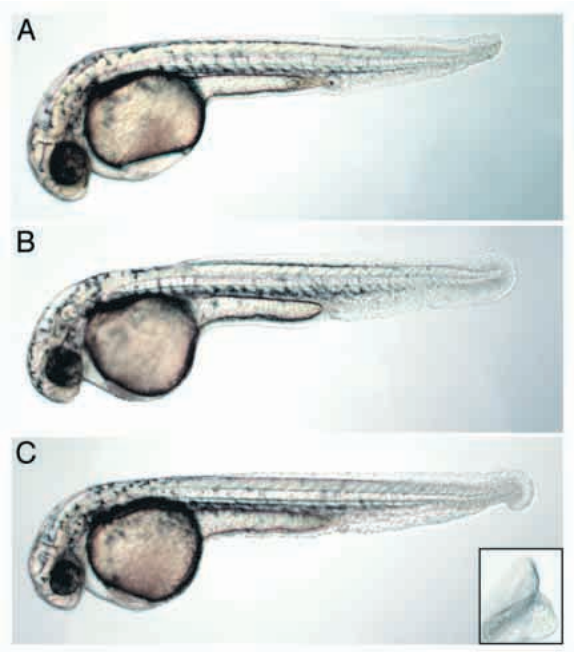

Fig. 1. Injection of *tld* mRNA rescues the *mfn* mutant phenotype. (A) An uninjected *mfn* mutant embryo displays a partial loss of the ventral tail fin. Embryos injected with *tld* mRNA can be rescued to wild-type (B) or a weakly ventralized phenotype (C) as indicated by a duplicated ventral tail fin tip (inset, posterior view). The phenotype in C is also observed in wild-type embryos ventralized by overexpression of *tld* (data not shown).

throughout the genome (Knapik et al., 1996, 1998). Marker Z1705 on linkage group 1 (LG1) appeared linked to *mfn* in pooled F_2 mutant DNA (data not shown). Linkage analysis in individual F_2 mutant embryos placed *mfn* approximately 3 cM from marker Z1705 (5 recombinants in 156 meioses, Fig. 2A,B). Examination of markers distal and proximal to Z1705 suggests that the *mfn* gene lies between Z1705 and Z1463, 1 to 3 cM from Z1463 (see Materials and Methods).

To establish the chromosomal position of the *tld* gene, we used a collection of zebrafish/mouse somatic cell hybrid (Ekker et al., 1996) and radiation hybrid (RH) panels (N. A. Hukriede, L. Joly, M. Tsang, J. Miles, P. Tellis, J. A. Epstein, W. B. Barbazuk, F. N. Li, B. Paw, J. H. Postlethwait, T. J. Hudson, L. I. Zon, J. D. McPherson, M. Chevrette, I. B. Dawid, S. L. Johnson and M. Ekker, personal communication). Of 94 somatic cell hybrid lines tested, six were positive for the *tld* gene, five of which have one or more known markers on LG1 (Fig. 2B). Examination of LG1 markers suggests that *tld* is found in an interval that separates markers Z1463 and Z3705. Linkage to microsatellite markers from this chromosomal region using the RH panel indicated a strong linkage between *tld* and Z1463 (LOD=20; 4.0 cR). Based on a preliminary estimate of the average breakpoint frequency of this RH panel (Hukriede et al., personal communication), *tld* would be within a Mbp from Z1463. To directly determine the proximity of *tld* to the *mfn* mutation, we examined linkage between an RFLP in the *tld* gene and the *mfn* mutation. We found no recombinants between the RFLP and the *mfn* mutation in 160 meioses (Fig. 2C), confirming that the *mfn* mutation is very closely linked to the *tld* gene, likely within 1 cM. Thus *tld* is an excellent candidate for the gene mutated in *mfn*.

mini fin is a mutation in the *tolloid* gene

To determine if *mfn* is a mutation in the *tld* gene, we cloned and sequenced *tld* cDNA clones from five of the nine *mfn* alleles. The zebrafish *tld* gene is predicted to encode a 1023 amino acid secreted protein constituting an amino-terminal signal sequence and pro-domain, followed by a metalloprotease domain, five CUB domains and two EGF repeats positioned between the CUB domains (Fig. 2D; Blader et al., 1997). The CUB domains and the EGF repeats are both thought to mediate protein-protein interactions (reviewed in Davis, 1990). Here we report on the identification of mutations in the five *mfn* alleles examined.

Nonsense mutations were identified in three *mfn* alleles. In the mfn^{tm124a} allele, a point mutation changes amino acid 181 from a glycine residue to a stop codon (Fig. 2D). This mutation occurs in the amino-terminal region of the metalloprotease domain, resulting in a predicted truncated protein missing both the functional metalloprotease and the protein-protein interaction domains. We expect this mutation is a strong loss-of-function allele, very likely a null mutation.

Stop codons were also found within the first and second CUB domains in mfn^{tb241c} and mfn^{tf215a}, respectively (Fig. 2D). Although the active site of the *tld* protein, the metalloprotease domain, is present in the predicted mutant proteins, the putative protein-protein interaction domains are mostly absent in these two alleles. Therefore, these proteins may not recognize and cleave their target, Chd.

We identified missense mutations within the mfn^{tn217b} and mfn^{ty130a} alleles (Fig. 2D). The mfn^{tn217b} mutation alters a leucine residue to proline at position 429 in the first CUB domain. Proline residues are known to disrupt certain secondary structures of proteins. This mutation occurs in a region proposed to form a β-strand (Bork and Beckmann, 1993) and may alter the Tld protein conformation. The mfn^{ty130a} allele changes a highly conserved cysteine in the metalloprotease domain to a tryptophan residue. In the Astacin protease, this cysteine forms an intramolecular disulfide bridge with a cysteine located 20 amino acids carboxy-terminal to it (Stöcker et al., 1993; Bode et al., 1992). Since these cysteine residues are invariant within the astacin protease family, it is likely that the disulfide bridge is present in all family members (Stöcker et al., 1993). The mfn^{ty130a} mutation would disrupt this disulfide bond, thus altering the Tld protein conformation.

The *mini fin* mutant phenotype

We have further characterized the *mfn* mutant phenotype to ascertain the function of *tld/mfn* in the zebrafish embryo. The recessive *mfn* phenotype is the weakest (class 1) of five dorsalized phenotypes identified in a large-scale mutant screen (Mullins et al., 1996). The phenotype is first morphologically discernible in some *mfn* mutant embryos at the bud stage (end of gastrulation) by a slight thickening of cells in the tail bud or a slightly ovoid shape of the embryo (Fig. 3A,B). By the 3-somite stage, all mutant embryos exhibit an abnormally shaped tail bud (Fig. 3C,D), which is reduced in length (arrows) and protrudes away from the yolk (asterisk). This phenotype contrasts with the ventralized mutant phenotypes of *chordino*

and *mercedes* embryos, which display a broader and flattened tail bud (Fisher et al., 1997; Hammerschmidt et al., 1996a). During later stages of somitogenesis, the tail bud of *mfn* mutant embryos continues to protrude abnormally away from the yolk (data not shown, Mullins et al., 1996).

At 24 hpf, *mfn* mutants display a range of phenotypes, which we divided into five categories (A-E) based on the degree to which ventral tail tissues are reduced. We established these categories to investigate the relative strengths of the different *mfn* alleles. The strongest *mfn* phenotype, category E, exhibits a complete loss of the ventral tail fin, frequently associated with reductions in caudal tail vasculature and ventral somitic mesoderm (Fig. 3H). Category D mutant embryos display a loss of more than half of the ventral tail fin (Fig. 3F), while in category C mutants half or less than half of the fin is absent (Fig. 1A). Category C and D mutant embryos occasionally exhibit a bifurcation of the tail (Fig. 3G). Category B mutants display an obvious notch in the ventral tail fin, while category A mutants exhibit a subtle reduction or small split in posterior ventral tail fin tissue (data not shown).

We used the criteria above to categorize mutant embryos of the nine *mfn* alleles and compare the strengths of their mutant phenotypes. We found that mutants of most alleles, including the presumptive null allele, mfn^{tm124a}, exhibit all categories (A-E) of phenotypes but to different degrees (Fig. 4). Our results suggest that there may be stronger (mfn^{ty130a} andmfn^{tm124a}) and weaker (mfn^{tt203} and mfn^{tf211a}) *mfn* alleles. However, since a complete range of phenotypes is observed in a putative null allele, the significance of the different phenotypic strengths for the various alleles is difficult to ascertain. The range of defects for a particular allele could reflect different degrees of compensatory regulation in mutant embryos. The strength of the phenotype could also be influenced by differences in genetic background. Further analysis of the strength of the *mfn/tld* mutations will require a biochemical determination of residual Tld activity. Interestingly, mutants of the Tld substrate, Chordin, also display a range of ventralized phenotypes at 24 hpf (Hammerschmidt et al., 1996a). Together with our analysis of *mfn*, this suggests some compensatory regulation occurring in modulating Bmp signaling levels.

Fish homozygous mutant for *mfn* are semiviable. Some mutant embryos survive to adulthood and appear nearly wild type (Fig. 3I) or are shorter in length and lack all or part of their tail and anal fins (Fig. 3J). In crosses with *mfn* homozygous females, no maternal-effect phenotype was detected.

Reduction in multiple ventral tail cell types in *mini fin* mutants

To investigate whether the ventral somitic mesoderm, vasculature and tail fin defects of *mfn* mutant embryos are due to a reduction of these tissues rather than their abnormal morphology, we examined several genes specifically expressed in these tissues. The *msxD* gene is expressed in the prospective median fin fold tissue by the 6-somite stage,

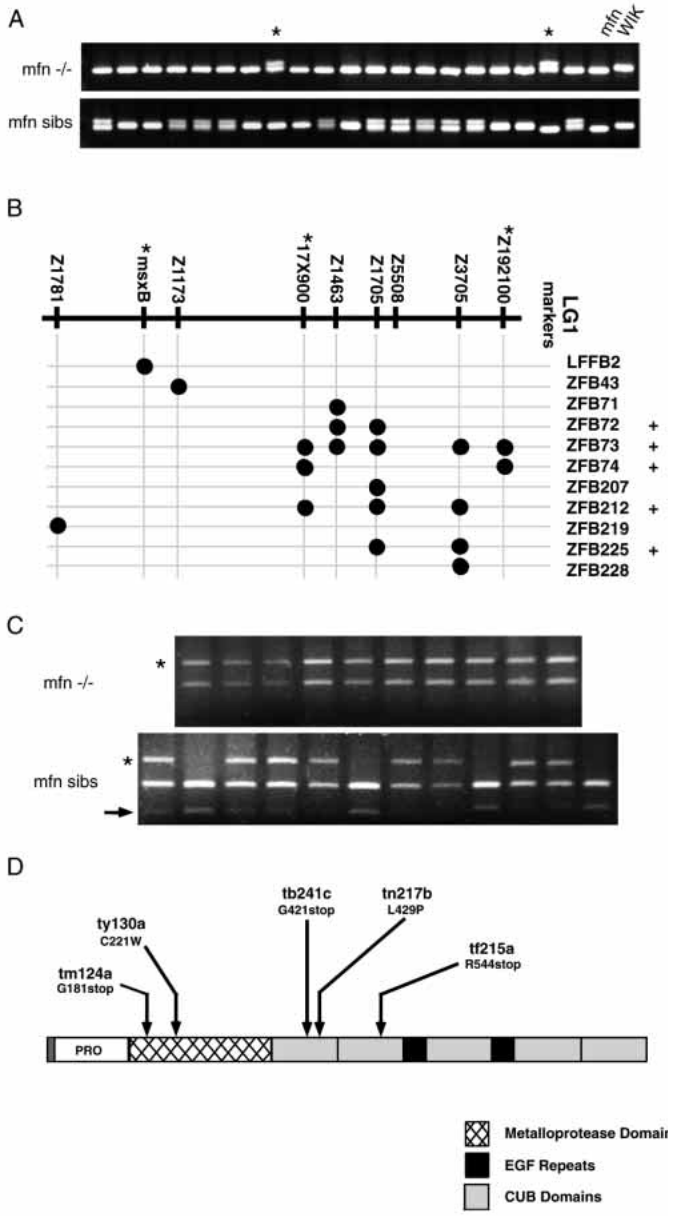

Fig. 2. SSLP mapping, RFLP linkage analysis, somatic cell hybrid screening, and sequence analysis show that *mfn* is a mutation in the *tld* gene. (A) Amplification of SSLP marker Z1705 from DNA of the G_0 mapping cross founder fish (TÜ-*mfn* and WIK) is shown in the last two lanes of each gel. DNA from most single F_2 *mfn* mutant embryos shows the TÜ-*mfn*-specific band, demonstrating linkage between the *mfn* mutation and Z1705. Two embryos show both bands (*), representing recombinant embryos between the Z1705 marker on the WIK chromosome and the *mfn* allele. Wild-type F_2 sibling embryo DNA shows either the WIK specific band (+/+ genotype) or both bands (+/– genotype). (B) Mapping of the *tld* gene in somatic cell hybrid lines places *tld* on LG1. Eleven hybrid lines containing portions of LG1 are listed in the right column. Five of these lines tested positive for the *tld* gene (+), placing *tld* between Z1463 and Z3705, in close proximity to the *mfn* mutation. The black circles indicate that a hybrid line is positive for that marker. The (*) indicates the markers that may not be to scale. (C) The *mfn* mutation is linked to an RFLP in the *tld* gene. The WIK allele contains an *Msp*I cleavage site in a 3′ UTR PCR product (arrow), which is absent in the TÜ-*mfn* allele (*). DNA from all single homozygous *mfn* F_2 embryos examined displayed the TÜ-*mfn* RFLP. Wild-type siblings show the TÜ-*mfn* and WIK RFLPs. (D) Schematic representation of the Tld protein and *mfn* mutations. ‘PRO’ is the presumptive pro-domain, which is thought to be cleaved off to form the active protease.

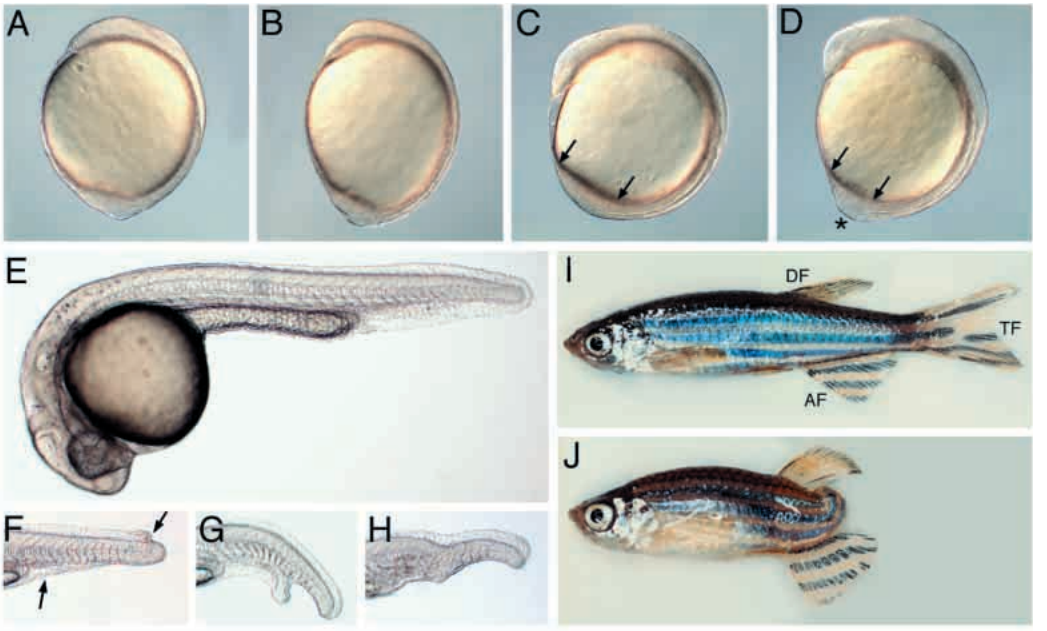

Fig. 3. Morphological defects visible in live *mini fin* mutant embryos. (A,B) 1-somite-stage *mfn* mutant (B) displays an oblong shape relative to wild type (A). 5-somite-stage wild-type (C) and *mfn* (D) mutant embryos. Arrows denote the tail bud length and the asterisk marks a protrusion of the tail bud seen in the mutant (D). 24 hpf wild type (E) and tails of *mfn* mutants exhibiting (F) a partial loss of tail fin (between the arrows) that extends to the dorsal side, (G) partial loss of the ventral fin with a bifurcation in the tail, (H) near complete absence of ventral fin and a kink in the tail. This occasionally observed kink is associated with a disruption in the notochord, which is also observed in the more strongly dorsalized mutant *lost-a-fin* (Solnica-Krezel et al., 1996, our unpublished observations). (I,J) *mfn* homozygous adult fish. Homozygous adult exhibiting a near wild-type appearance (I). Note that a pigmented stripe in the tail is disrupted in this mutant, a trait characteristic of *mfn* homozygous fish. Other adult mutants may display a partial or full (J) loss of their tail fin. All are lateral views. (A-D) dorsal to the right, (E-J) dorsal to the top. AF, anal fin; TF, tail fin; DF, dorsal fin.

specifically labeling cells at the caudal tip of the embryo (Akimenko et al., 1995). In 8-somite-stage *mfn* mutants, *msxD* expression was reduced or absent (Fig. 5A,B). At the 14-somite stage, the *msxB* and *dlx3* genes are also expressed in cells of the presumptive median fin fold (Akimenko et al., 1994, 1995). In *mfn* mutants, a gap in expression is observed caudal to the tail bud (Fig. 5C,D, data not shown). At 24 hpf, the expression patterns of these genes correspond precisely to the phenotypes observed in live mutant embryos (compare Fig. 3F-H with Fig. 5F-H, respectively). Thus, the reduction in the ventral tail fin at 24 hpf in *mfn* mutant embryos is apparent as early as the 8-somite stage by a loss of prospective fin fold tissue.

Many *mfn* mutants fail to establish normal blood circulation. To investigate whether a loss of vasculature is associated with this defect, we examined the expression of *flk1*, a marker for vascular endothelial cells (Fouquet et al., 1997; Liao et al., 1997; Thompson et al., 1998). The degree to which the *flk1* expression pattern was altered typically corresponded to the severity of the *mfn* mutant phenotype. At 24 hpf, weak *mfn* mutant embryos displayed normal *flk1* expression (data not shown). An aberrant *flk1* expression pattern was observed in some *mfn* mutants (Fig. 5J), which may reflect an abnormal morphology and/or reduction in *flk1* expression. Other *mfn* mutant embryos displayed a reduction of *flk1* expression in caudal regions of the tail (Fig. 5K), indicating that the loss of vasculature observed in some *mfn* mutants is due to a reduction in the number of endothelial precursor cells.

We analyzed *myoD* expression (Weinberg et al., 1996) at 24 and 32 hpf to examine tail somite formation in *mfn* mutant embryos. Weak and most of the moderate strength *mfn*

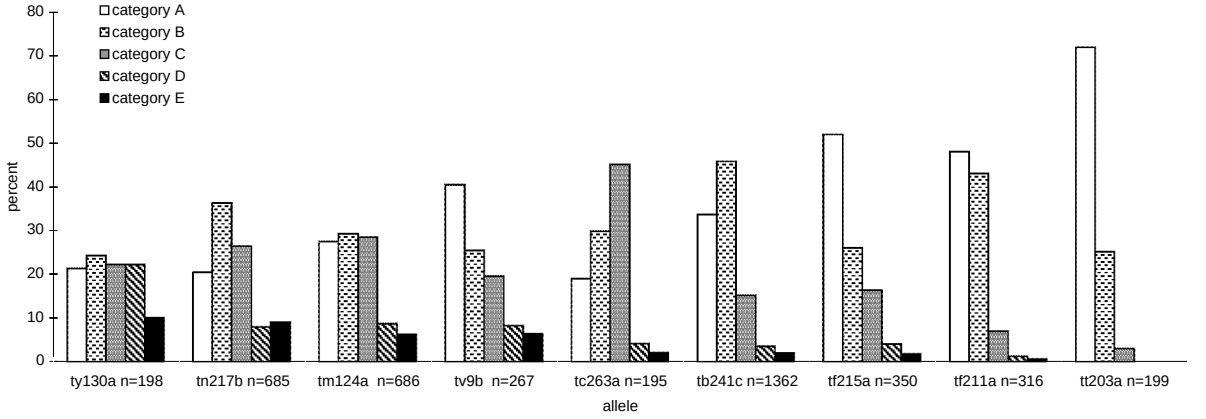

Fig. 4. Analysis of *mfn* allele strengths. *mfn* mutant embryos were divided into five categories (A-E) as described in the text. Category A represents the weakest phenotypic class and category E the strongest.

mutant embryos (category A-D) display a normal *myoD* expression pattern (data not shown). Moderate *mfn* mutant embryos (category C, D) with a bifurcated tail tip frequently contain somitic tissue in both forks (Fig. 5N). Stronger *mfn* mutant embryos (category E with kinked tails) usually lack or exhibit a reduction in ventral somitic tissue posterior to the bent notochord (Fig. 5M and data not shown). The partial loss of three ventral tissue types of the tail, somitic mesoderm, blood vessel endothelial cells and fin tissue suggests that *mfn* does not act in the specification of a particular cell type, but rather functions in establishing the pattern of ventral tail tissues.

mini fin/tolloid functions by the end of gastrulation in ventral regions

Vasculature and ventral tail fin tissue have been fate mapped to ventral regions of the blastula or gastrula embryo (Lee et al., 1994; Woo and Fraser, 1998). Since these tissues are reduced or absent in *mfn* mutant embryos, we investigated whether these losses are reflected at earlier stages in development in the altered expression of markers of ventral regions. We examined the expression of *eve1* (Joly et al., 1993) and *bmp4* (Chin et al., 1997; Nikaido et al., 1997), which are expressed in ventral (or posterior) tissue from mid-gastrulation through somitogenesis stages. Analysis of *eve1* and *bmp4* expression in *mfn* mutant gastrula (80-90% epiboly) did not reveal a clear reduction of ventral cell fates. We detected a smaller domain of *eve1* and *bmp4* expression in a small fraction of embryos (<10%) in some broods. We genotyped these embryos and found that embryos with the most severely reduced expression correlated to *mfn* homozygous mutant embryos, but we also found a small fraction of wild-type embryos with slightly reduced domains (data not shown).

By the bud stage, however, many *mfn* mutant embryos display a reduction in *eve1* expression (Fig. 6A,B) and the posterior (or ventral) *bmp4* expression domain (Fig. 6C,D) within the tail bud. These markers, which continue to be expressed in the extending tail bud during somitogenesis stages, remain reduced in all *mfn* mutant embryos (data not shown). Thus, *mfn/tld* may act during late gastrulation and is clearly functioning at the end of gastrulation. Moreover, these data indicate that *tld* specifies tissues of ventral character within the tail bud.

Expression pattern of *tolloid/mini fin*

We examined the expression pattern of *tld* from early gastrulation to 24 hpf to investigate how *tld* expression may account for its role in ventral or posterior cell fate specification. From the shield to bud stages, *tld* is expressed at a low level with a spotty appearance in superficial cells in both dorsal and ventral animal pole regions (Fig. 6E,F and data not shown). At 55% epiboly, a clearing is observed in a dorsal quadrant, except for expression close to the edge of the margin (Fig. 6E). At 70% epiboly, *tld* is expressed uniformly in ventral regions in cells below the superficial clusters and strongly around the margin (Fig. 6G), similar to earlier stages (Fig. 6E). At 80-90% epiboly, the ventral domain no longer extends to the margin, but instead lies in the animal half of the embryo (Fig. 6H). As previously reported (Blader et al., 1997), at the bud stage *tld* expression is observed transiently along the edge of the neural plate and the marginal *tld* expression domain now appears to lie within the tail bud (Fig. 6I), where it continues to be strongly expressed during somitogenesis stages (Fig. 6J,K). By 20 somites, *tld* is expressed in prospective vascular tissue (Fig. 6J), similarly to *flk1*. Thus, the expression of *tld* within the margin late in gastrulation and within the tail bud is consistent with a role for *tld* in the establishment of ventral tail cell fates.

Regulation of *tolloid* gene expression by *chordin* and *bmp2b*

Bmp2 and *Bmp4* gene expression is under the control of an autoregulatory feedback mechanism (Jones et al., 1992; Kim

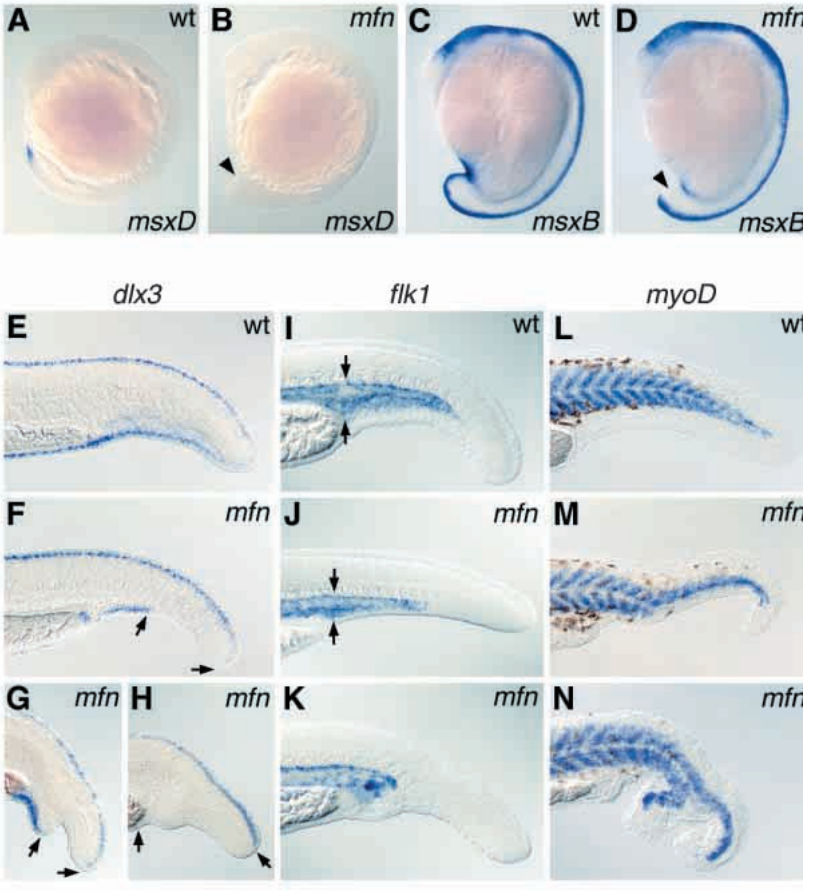

Fig. 5. Absence or reduction of three ventral tail cell types in *mfn* mutants. *msxD* expression in 8-somite-stage wild-type (A) and *mfn* mutant (B) embryos. *msxB* expression in 14-somite-stage wild-type (C) and *mfn* mutant (D) embryos. *msxB* is also expressed in other more anterior cell types. *dlx3* expression in 24 hpf wild-type (E) and mutant (F-H) embryos. *flk1* expression in 24 hpf wild-type (I) and mutant (J,K) embryos. Note reduced *flk1* in *mfn* (arrows). *myoD* expression in 32 hpf wild-type (L) and mutant (M,N) embryos. Arrowheads in B and D denote reduced/absent gene expression in the mutant. (F-H) Ventral *dlx3* expression is absent between the arrows. All are lateral views. (A-D) Dorsal is to the right, anterior to the top. (E-N) Dorsal is to the top, anterior to the left.

et al., 1998; Kishimoto et al., 1997; Metz et al., 1998; Nguyen et al., 1998b), while *chordin* expression is negatively regulated by Bmp signaling (Miller-Bertoglio et al., 1997; Schulte-Merker et al., 1997). To examine whether *tld* gene expression is regulated similarly to the *Bmp* ligand genes, we examined *tld* expression in *chordino* and *swirl* mutant embryos. In *chordino* mutants at bud stage and throughout somitogenesis stages, the tail bud expression domain of *tld* is broadened relative to wild type (Fig. 6K,L, and data not shown). In *swirl/bmp2b* dorsalized mutant embryos, *tld* expression is reduced at bud and later stages (Fig. 6M, data not shown). Thus, *tld* gene expression at these stages is regulated positively by *bmp2b/swirl* and negatively by *chd*.

Pattern of *tolloid/mini fin* expression relative to *chordin* and *bmp4*

We investigated the spatial relationships of the *chd*, *tld* and *bmp4* expression domains at the bud stage, when we know *mfn/tld* functions, to examine possible functional relationships between these genes. Double in situ hybridizations of *chd*, *tld* and *chd*, *bmp4* at the bud stage in wild-type embryos shows that *tld* and *bmp4* expression is excluded from the more anteriorly located *chd* expression domain (Fig. 6N,O). Moreover, *tld* expression lies adjacent to the *chd* expression domain, while a prominent gap is found between the *bmp4* and *chd* expression domains. The *bmp4* gene expression domain extends further laterally and posteriorly than does *tld* (data not shown) and *tld* expression lies closer to the anterior side of the tail bud than does *bmp4*. Thus *tld* mRNA is in the correct location for Tld to play a role in modulating presumptive Bmp4 activity levels through cleavage of Chd.

We examined the involvement of *tld/mfn* in shaping the *chd* and *bmp4* expression domains. At the bud stage, *chd* expression is expanded posteriorly and laterally in some *mfn* mutants (Fig. 6O,P), while *tld* and *bmp4* expression domains are reduced in all mutant embryos (Fig. 6O,P and C,D, respectively). At the 7-somite stage, an expansion of *chd* is also observed in some, but not all, *mfn* mutants, which likely reflects the strength of the *mfn* mutant phenotype. It is possible that the range of *mfn* mutant phenotypes is caused, in part, by the degree to which *chd* gene expression is expanded. Altogether, these results are consistent with Tld positively modulating Bmp signaling levels, which is then reflected in the positive regulation of *bmp4* and *tld* gene expression and negative regulation of *chd* expression.

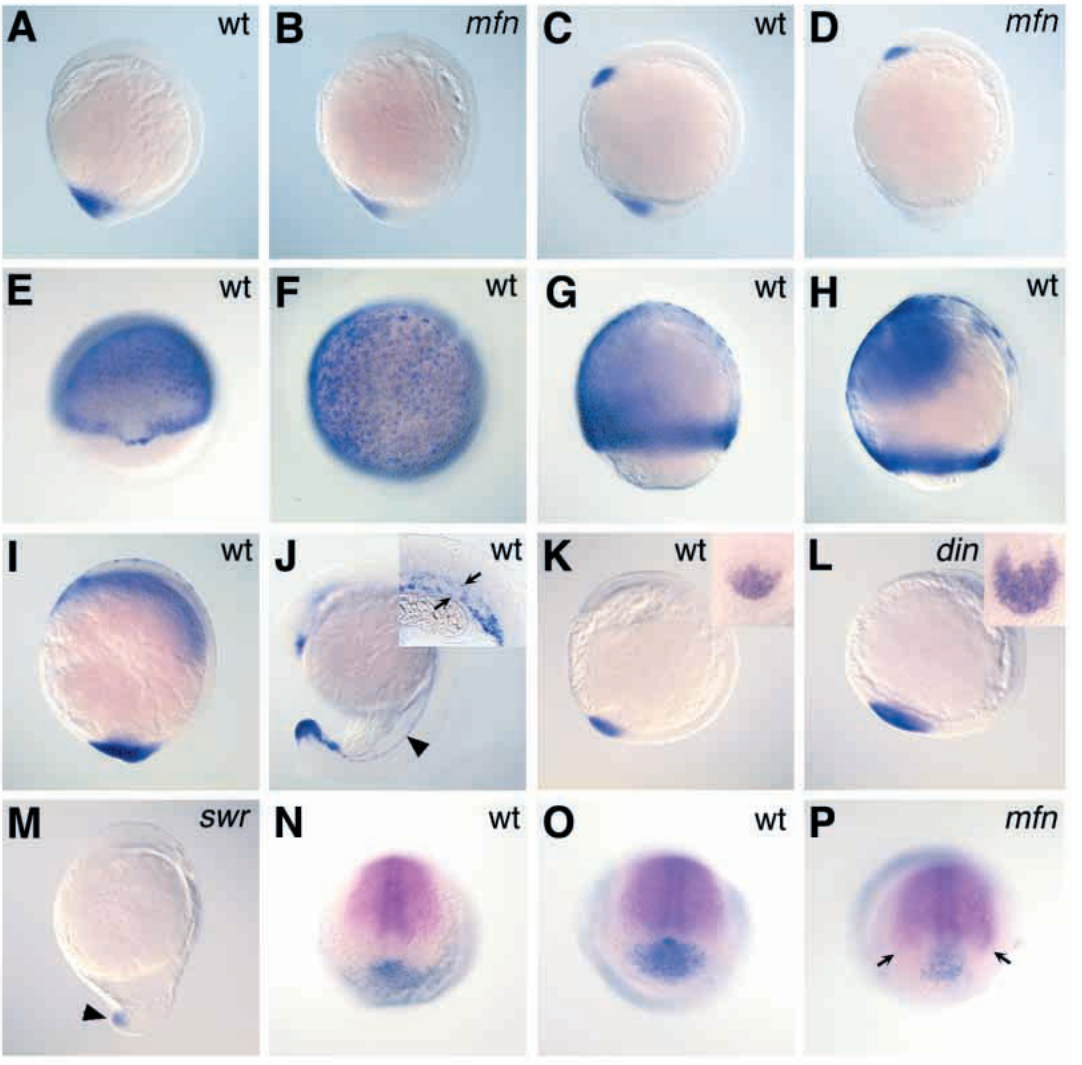

Fig. 6. *tld* expression pattern and altered *tld*, *chd* and *bmp4* expression in mutant embryos. *eve1* expression in bud stage wild-type (A) and *mfn* mutant (B) embryos. *bmp4* expression in 1-somite-stage wild-type (C) and *mfn* mutant (D) embryos. *tld* expression in wild-type embryos at 55% epiboly (E), 70% epiboly (F,G), 85% epiboly (H), bud-stage (I) and 20-somite-stage (J) wild-type embryos. Arrowhead in J points to *tld* expression in the presumptive vasculature. Inset in J is a higher magnification showing the posterior trunk of a slightly older embryo with *tld* expression marking the prospective artery and vein (arrows). *tld* expression at 5 somites in wild-type (K), *chordino* (L) and *swirl* (M) mutant embryos. Insets in K-L are higher magnification caudal views of *tld* expression, anterior to the top. Reduced *tld* expression (arrowhead) in a *swirl* mutant. Double in situ of *chd* (magenta) and *bmp4* (blue) expression in a bud-stage wild-type embryo (N). Double in situ of *chd* (magenta) and *tld* (blue) expression in bud-stage wild-type (O) and *mfn* mutant (P) embryos. (P) Expanded *chd* expression (arrows) in a *mfn* mutant. (A-D, G-M) Lateral views, dorsal to the right. (E) Dorsal view, slightly tilted downward. (F) Animal pole view. (N-P) Vegetal pole view, anterior/dorsal to the top.

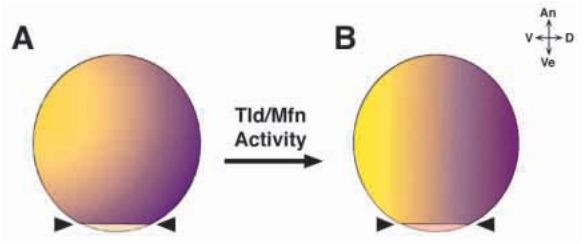

Fig. 7. One model of Tld function. (A) If Chordin (purple) can diffuse unimpeded across the embryo, the smaller marginal diameter (arrowheads) at late gastrulation stages may result in Chordin reaching the ventral side in vegetal regions (left arrowhead). This would result in a decrease in the ventralmost Bmp activity (yellow). (B) Tolloid, which is expressed strongly vegetally in the margin (see Fig. 6H), would act to increase ventral Bmp activity by cleaving Chordin, thus allowing for specification of ventral tail tissues. D, dorsal; V, ventral; An, animal pole; Ve, vegetal pole.

DISCUSSION

mini fin encodes *tolloid* and specifies ventral tail cell fates

We have shown that *mini fin* encodes the *tolloid* gene, based on three lines of evidence. First, overexpression of *tld* mRNA specifically rescues *mfn* mutants to a wild-type phenotype. Second, *tld* and *mfn* are very closely linked in the zebrafish genome. Lastly, three stop codon and two missense mutations were found in the five *mfn* alleles analyzed, verifying that *mfn* encodes *tld*.

The *mfn* phenotype is characterized by a partial to complete loss of the ventral tail fin, and a reduction in caudal tail vein and somitic mesoderm in strong mutant embryos. The reduction in three different ventral tail tissues suggests that *mfn* is not involved in the differentiation or specification of a particular cell type, but rather may act in the establishment of the general pattern of the tail. Vasculature and ventral tail fin tissues have been fate mapped to ventral regions of blastula (Lee et al., 1994) and mid-gastrula (Woo and Fraser, 1998) embryos, respectively, suggesting that ventral cell fate specification is affected in *mfn* mutant embryos. A reduction in the expression of two markers of ventral tissue at the end of gastrulation in *mfn* mutants supports such a role for *mfn/tld*. Additional results and observations, as discussed below, add strength to the hypothesis that *mfn*/*tld* normally is involved in the specification of ventral cell fates at the end of gastrulation in the zebrafish embryo, likely by increasing Bmp activity.

Similarity between *mini fin* and *swirl* phenotypes

Phenotypes identical to those of *mfn* mutants are observed in other dorsalized mutant embryos, including dominant phenotypes of *swirl*/*bmp2b* (Mullins et al., 1996). Characterization of homozygous *swirl* mutant gastrula shows that *swirl* is involved in the specification of nearly all ventral cell fates (Nguyen et al., 1998b). The presumed reduction in Bmp2b activity in *swirl* heterozygotes produces a partially penetrant phenotype, suggesting that Bmp2b activity is at a threshold level for normal development in these mutant embryos. Interestingly, this partial loss of *bmp2b* gene activity results in a weak dorsalization identical to the *mfn*/*tld* phenotype described here. Since Tld can enhance Bmp activity through the cleavage and inactivation of Chd (Blader et al., 1997; Marqués et al., 1997; Piccolo et al., 1997), loss-of-function mutations in *tld* are expected to decrease Bmp activity. The similarity in the dominant loss-of-function *swirl/bmp2b* phenotype to the *mfn/tld* mutant phenotype strongly supports a role for *mfn/tld* in increasing Bmp activity in ventroposterior cells, which then specifies ventral tail cell fates.

Feedback regulation of *tolloid*, *chordin* and *bmp* expression

In frog and fish embryos, *bmp2* and *bmp4* gene expression is under the control of an autoregulatory mechanism (Jones et al., 1992; Kim et al., 1998; Kishimoto et al., 1997; Metz et al., 1998; Nguyen et al., 1998b). Chd can negatively regulate *bmp* gene expression (Hammerschmidt et al., 1996b; Kim et al., 1998; Metz et al., 1998), presumably by inhibiting Bmp activity and interrupting the autoregulatory feedback loop. In a reciprocal manner, Bmp activity can negatively regulate *chd* gene expression (Miller-Bertoglio et al., 1997; Schulte-Merker et al., 1997). Consistent with a role for Tld in modulating Bmp activity, we observe a reduction in the domain of *bmp4* gene expression and an expansion of *chd* gene expression in *mfn/tld* mutants. Tld likely regulates *bmp* gene expression by cleaving Chd, thus increasing Bmp activity, which would then induce additional *bmp* transcription through the autoregulatory loop. The expression of *tld* may also be part of this feedback regulatory loop, since *tld* gene expression is expanded in *chordino* mutants and reduced in *swirl* mutants.

The role of Tolloid in early gastrulation

Our analysis of the *mfn/tld* mutant phenotype indicates that Mfn/Tld plays little or no role during early gastrulation in the zebrafish, although it is expressed at this time. We discuss two alternative hypotheses for this lack of *mfn/tld* function. The first hypothesis is that a second *tld*-related gene in zebrafish exists and acts redundantly to *mfn/tld*. It is likely that additional *tld*-related genes are present in the zebrafish, since two *tld*-related genes have been identified in the mouse, human and frog. In *Xenopus*, for example, *Xolloid* (*Xld*) and one long splice variant from the *Bmp1* locus, called *Xtolloid* (*XTld*), have been reported (Goodman et al., 1998; Lin et al., 1997). Overexpression of a dominant-negative form of *Xolloid* (DN-*Xld*) moderately dorsalizes anterior tissue of the *Xenopus* embryo (Piccolo et al., 1997), suggesting an early function for Xld during gastrulation (Piccolo et al., 1997). *Xld*, however, is not detectable by whole-mount in situ hybridization during gastrulation, arguing against it functioning at these stages (Goodman et al., 1998). At least one of the transcripts from the *Bmp1* locus is expressed during gastrulation (Goodman et al., 1998; Lin et al., 1997) and could be the activity inhibited by the DN-*Xld*. Overexpression of a DN-*tld* in the zebrafish causes a low frequency of predominantly weak dorsalization phenotypes (Blader et al., 1997), inconsistent with *mfn/tld* or another *tld* gene playing a significant role early in gastrulation. However, it is possible that the zebrafish DN-*tld* is not as effective as the frog DN-*Xld*, which contains a different mutation. The mechanisms by which the DN-Tld/Xld act are not understood, leaving open the possibility that Bmp activity is reduced by the DN-Xld, independent of normal Tld function.

Further experimental analysis is required to establish whether Tolloid inhibits Chordin activity during early gastrulation.

An alternative hypothesis for the lack of detectable *mfn/tld* function early in gastrulation is that neither Mfn/Tld nor another Tld-related protein inhibits Chordin activity at these stages. It is possible that the large circumference of the zebrafish embryo is sufficient to generate the necessary Bmp activity gradient through the presumed diffusion of dorsally expressed Chordin and other Bmp antagonists into ventral regions. A corollary to this hypothesis could explain the more severe defects observed in the fly *tld* mutant compared to the zebrafish *mfn* mutant. Null mutant *tld* embryos in the fly are lethal and exhibit a moderate ventralization, affecting the dorsal ~25% of the fate map (Arora and Nüsslein-Volhard, 1992), compared to the weak semiviable dorsalization of the *mfn* mutant. The smaller circumference of the fly embryo, ~630 μm (Ashburner, 1989) compared to 2200 μm in the zebrafish (Kimmel et al., 1995), may necessitate a more prominent role for the fly Tld in repressing Sog function in dorsal regions. Sog appears to diffuse at least 12 to 15 cell diameters (Biehs et al., 1996), or up to 120 μm, from its ventral expression domain and may diffuse to the most dorsal point of the fly embryo, ~135 μm. A function of the fly Tld, which is expressed in the dorsal 40% of the embryo, may be to restrict Sog repressive action in the dorsalmost regions in order to generate the necessary Bmp activity gradient. In zebrafish, this gradient may be established during early gastrulation solely by diffusion of Chd, and possibly other Bmp antagonists, independent of Tld function.

The role of Tolloid/Mini fin in late gastrulation and tail bud stages

The first consistent alteration in *mfn/tld* mutant embryos is apparent at the time of tail bud formation at the end of gastrulation (the bud stage), indicating that *tld/mfn* functions at least by this stage. Since *tld* is strongly expressed within the posterior tail bud, we hypothesize that *tld/mfn* functions within the tail bud itself in the specification of ventral tail cell fates. Similarly, *Xld* may also play a role in ventral cell fate specification within the *Xenopus* tail bud, since its expression is specifically localized to prospective tail cell types at neurula and later stages (Goodman et al., 1998; Piccolo et al., 1997).

Previous studies based on analysis of cell movements and gene expression domains within the tail bud suggest that tail formation results from a modified form of gastrulation in the tail bud (Catala et al., 1995; Gont et al., 1993; Kanki and Ho, 1997; Knezevic et al., 1998; Pasteels, 1943; Tucker and Slack, 1995). Anterior and posterior domains of the tail bud express genes that are dorsally and ventrally restricted in gastrulation, respectively (Gont et al., 1993). Fate map data also support a restriction of dorsally derived gastrula cell fates to the anterior tail bud (Kanki and Ho, 1997). Moreover, cell transplantation experiments between anterior and posterior tail bud regions indicate that cells of the tail bud are not determined at the bud stage (Kanki and Ho, 1997; J. Kanki, personal communication). Hence, the juxtaposed expression domains of *chd* to *bmp4* and *tld* within the tail bud suggests that these genes may function in patterning prospective tail tissues from the bud stage onwards.

We propose that Tld/Mfn function is crucial during late gastrulation and tail bud stages to repress Chd activity. At these stages, the ventralmost vegetal cells of the late gastrula and tail bud lie in close proximity to the dorsal-expressing Chordin cells. It is conceivable that at these stages Chordin could diffuse, if unimpeded, to the ventralmost regions and inhibit Bmp signaling (Fig. 7). We hypothesize that the high expression of *tld* in the margin of the late gastrula and within the tail bud acts to limit Chd activity, thereby increasing Bmp activity, which then specifies ventral tail cell fates. When functional Tld/Mfn is reduced in the embryo, higher levels of Chd are expected to cause a reduction in Bmp activity. This would then affect the transcriptional autoregulatory loop of *bmp* and *chd* gene expression, further decreasing Bmp activity and expanding the domain of Chd antagonism. Consequently, the Bmp activity levels required for ventral tail cell fate specification are not attained, resulting in the loss of ventral tail tissues.

Remaining questions

We cannot yet account for two potential modes of spatial regulation of Tld activity. First, Tld is processed from its zymogen form to an active protease (Marqués et al., 1997; Piccolo et al., 1997). In the fly embryo, only a small fraction of Tld is processed by a yet unknown mechanism (Marqués et al., 1997). Likewise, in vertebrate embryos, it is not known how Tld is processed and if it is regulated in some manner. Second, in tissue culture experiments, the fly Tld cleaves Sog much more efficiently when bound to Dpp (or other BMPs; Marqués et al., 1997; Nguyen et al., 1998a), while Xld and the zebrafish Tld can act on Chd alone (Blader et al., 1997; Piccolo et al., 1997) or in complex with BMPs (Piccolo et al., 1997). The kinetics of Tld cleaving Chd versus a Chd-Bmp complex and the endogenous requirements for cleavage have not been established. Hence, we make no assumption as to where in the margin or tail bud Tld cleaves Chd.

Graded Bmp activity appears to be established through the action of specific Bmp antagonists. It is clear that additional molecules, such as Tld, are also critical in modulating Bmp activity levels. The precise role played by Tld in the zebrafish and fly in regulating the Bmp activity gradient remains unclear. Its primary function may be to limit Chd/Sog activity in regions where the entire *bmp* expression domain lies near to the *chd/sog* expression domain, and Chd/Sog may diffuse across most or all of the *bmp* expression domain to inhibit most Bmp signaling (e.g. in the the tail bud of the zebrafish embryo and the dorsoventral axis of the fly embryo). Alternatively, it may be required to shape or refine the gradient in a particular manner to generate the readout necessary to specify different cell fates in particular domains. A further role of Tld may be in the generation of Sog/Chd cleavage products, which could play additional roles in development as suggested by Marqués et al. (1997). These and other questions remain to be resolved.

We thank Patrick Blader and Uwe Strähle for generously providing tolloid injection and in situ constructs, and Mark Fishman and Ela Knapik for kindly providing SSLP marker information prior to publication. We also thank Alvin Chin, Valarie Miller-Bertoglio, Marnie Halpern, Marie-Andrée Akimenko, Eric Weinberg, Jean-Stefan Joly, Didier Stainier and Len Zon for in situ probes, Dan Kessler, Steve DiNardo, Michael Granato, Dan Wagner, Bettina Schmid, Vu Nguyen and Keith Mintzer for critical review of the manuscript, and Andrea Payne and Chapell Miller for care of the fish. We thank Bettina Schmid for generation of homozygous *mfn* fish and Vu Nguyen for some expression data in *swirl* mutants. Special thanks

to Lucille Joly for help with mapping, Neil Hukriede for assistance with RH data analysis, and John Kanki for sharing unpublished observations. This work was supported by a grant from the NIH to M. C. M. (R01-GM56326), funding from the Medical Research Council of Canada to M. E., and training grants (T32 HD07305 and T32 HD07516 01) to S. A. C.

REFERENCES

Akimenko, M.-A., Ekker, M., Wegner, J., Lin, W. and Westerfield, M. (1994). Combinatorial expression of three zebrafish genes related to distal-less: Part of a homeobox gene code for the head. *J. Neurosci.* **14,** 3475-3486.

Akimenko, M. A., Johnson, S. L., Westerfield, M. and Ekker, M. (1995). Differential induction of four *msx* homeobox genes during fin development and regeneration in zebrafish. *Development* **121,** 347-357.

Arora, K. and Nüsslein-Volhard, C. (1992). Altered mitotic domains reveal fate map changes in *Drosophila* embryos mutant for zygotic dorsoventral patterning genes. *Development* **114,** 1003-1024.

Ashburner, M. (1989). *Drosophila: A Laboratory Handbook.* Cold Spring Harbor Laboratory Press,

Biehs, B., François, V. and Bier, E. (1996). The *Drosophila short gastrulation* gene prevents Dpp from autoactivating and suppressing neurogenesis in the neuroectoderm. *Genes Dev.* **10,** 2922-2934.

Blader, P., Rastegar, S., Fischer, N. and Strähle, U. (1997). Cleavage of the BMP-4 antagonist Chordin by Zebrafish Tolloid. *Science* **278,** 1937-1940.

Bode, W., Gomis-Rüth, F. X., Huber, R., Zwilling, R. and Stöcker, W. (1992). Structure of astacin and implications for activation of astacins and zinc-ligation of collagenases. *Nature* **358,** 164-167.

Bork, P. and Beckmann, G. (1993). The CUB Domain A Widespread Module in Developmentally Regulated Proteins. *J. Molec. Biol.* **231,** 539-545.

Catala, M., Teillet, M.-A. and Le Douarin, N. M. (1995). Organization and development of the tail bud analyzed with the quail-chick chimaera system. *Mech. Dev.* **51,** 51-65.

Chevrette, M., Joly, L., Tellis, P. and Ekker, M. (1997). Contribution of zebrafish-mouse cell hybrids to the mapping of the zebrafish genome. *Biochem. Cell Biol.* **75,** 641-649.

Chin, A. J., Chen, J. N. and Weinberg, E. S. (1997). *Bone morphogenic protein-4* expression characterizes inductive boundaries in organs of developing zebrafish. *Dev. Genes Evol.* **207,** 107-114.

Davis, C. G. (1990). The many faces of epidermal growth factor repeats. *New Biologist* **2,** 410-419.

De Robertis, E. M. and Sasai, Y. (1996). A common plan for dorsoventral patterning in Bilateria. *Nature* **380,** 37-40.

Dosch, R., Gawantka, V., Delius, H., Blumenstock, C. and Niehrs, C. (1997). Bmp-4 acts as a morphogen in dorsoventral mesoderm patterning in *Xenopus*. *Development* **124,** 2325-2334.

Ekker, M., Speevak, M. D., Martin, C. C., Joly, L., Giroux, G. and Chevrette, M. (1996). Stable transfer of zebrafish chromosome segments into mouse cells. *Genomics* **33,** 57-64.

Ferguson, E. and Anderson, K. (1992a). *Decapentaplegic* acts as a morphogen to organize dorsal-ventral pattern in the *Drosophila* embryo. *Cell* **71,** 451-461.

Ferguson, E. L. and Anderson, K. V. (1992b). Localized enhancement and repression of the activity of the TGF-β family member, *decapentaplegic*, is necessary for dorsal-ventral pattern formation in the *Drosophila* embryo. *Development* **114,** 583-597.

Fisher, S., Amacher, S. L. and Halpern, M. E. (1997). Loss of *cerebum* function ventralizes the zebrafish embryo. *Development* **124,** 1301-1311.

Fouquet, B., Weinstein, B. M., Serluca, F. C. and Fishman, M. C. (1997). Vessel patterning in the embryo of the zebrafish: guidance by notochord. *Dev. Biol.* **183,** 37-48.

Fukagawa, M., Suzuki, N., Hogan, B. L. and Jones, M. C. (1994). Embryonic expression of mouse bone morphogenetic protein-1 (BMP-1), which is related to the *Drosophila* dorsoventral gene *tolloid* and encodes a punative astacin metalloendopeptidase. *Dev. Biol.* **163,** 175-183.

Gates, M. A., Kim, L., Egan, E. S., Cardozo, T., Sirotkin, H. I., Dougan, S. T., Lashkari, D., Abagyan, R., Schier, A. F. and Talbot, W. S. (1999). A genetic linkage map for zebrafish: comparative analysis and localization of genes and expressed sequences. *Genome Res.*, in press.

Gont, L., Steinbeisser, H., Blumberg, B. and De Robertis, E. (1993). Tail formation as a continuation of gastrulation: the multiple cell populations of the *Xenopus* tailbud derive from the late blastopore lip. *Development* **119,** 991-1004.

Goodman, S. A., Albano, R., Wardel, F. C., Matthews, G., Tannahill, D. and Dale, L. (1998). BMP1-Related Metalloproteinases Promote the Development of Ventral Mesoderm in Early Xenopus Embryos. *Dev. Biol.* **195,** 144-157.

Graff, J. M. (1997). Embryonic patterning: To BMP or not to BMP, that is the question. *Cell* **89,** 171-174.

Hammerschmidt, M., Pelegri, F., Mullins, M. C., Kane, D. A., van Eeden, F. J. M., Granato, M., Brand, M., Furutani-Seiki, M., Haffter, P., Heisenberg, et al. and Nüsslein-Volhard, C. (1996a). *dino* and *mercedes*, two genes regulating dorsal development in the zebrafish embryo. *Development* **123,** 95-102.

Hammerschmidt, M., Serbedzija, G. N. and McMahon, A. P. (1996b). Genetic analysis of dorsoventral pattern formation in zebrafish: requirment of a BMP-like ventralizing activity and its dorsal repressor. *Genes Dev.* **10,** 2452-2461.

Hogan, B. L. (1996). Bone morphogenic proteins: mulitifunctional regulators of vertebrate development. *Genes Dev.* **10,** 1580-1594.

Joly, J. S., Joly, C., Schulte-Merker, S., Boulekbache, H. and Condamine, H. (1993). The ventral and posterior expression of the zebrafish homeobox gene *eve1* is perturbed in dorsalized and mutant embryos. *Development* **119,** 1261-1275.

Jones, C. M., Lyons, K. M., Lapan, P. M., Wright, C. V. E. and Hogan, B. L. M. (1992). DVR-4 (Bone morphogenetic protein-4) as a posterior-ventralizing factor in *Xenopus* mesoderm induction. *Development* **115,** 639-647.

Jones, C. M. and Smith, J. C. (1998). Establishment of a BMP-4 morphogen gradient by long-range inhibition. *Dev. Biol.* **194,** 12-17.

Kanki, J. P. and Ho, R. K. (1997). The development of the posterior body in zebrafish. *Development* **124,** 881-893.

Kim, J., Ault, K. T., Chen, H.-D., Xu, R.-H., Roh, D.-H., Lin, M. C., Park, M.-J. and Kung, H.-F. (1998). Transcriptional regulation of BMP-4 in the *Xenopus* embryo: analysis of genomic BMP-4 and its promoter. *Biochem. Biophys. Res. Commun.* **250,** 516-530.

Kimmel, C. B., Ballard, W. W., Kimmel, S. R., Ullmann, B. and Schilling, T. (1995). Stages of embryonic development of the zebrafish. *Dev. Dyn.* **203,** 253-310.

Kishimoto, Y., Lee, K. H., Zon, L., Hammerschmidt, M. and Schulte-Merker, S. (1997). The molecular nature of zebrafish *swirl*: BMP2 function is essential during early dorsoventral patterning. *Development* **124,** 4457-4466.

Knapik, E. W., Goodman, A., Atkinson, O. S., Roberts, C. T., Shiozawa, M., Sim, C. U., Weksler-Zangen, S., Trolliet, M. R., Futrell, C., Innes, B. A., et al. (1996). A reference cross for the zebrafish (*Danio rerio*) anchored with simple sequence length polymorphisms. *Development* **123,** 451-460.

Knapik, E. W., Goodman, A., Ekker, M., Chevrette, M., Delgado, J., Neuhauss, S., Shimoda, N., Driever, W., Fishman, M. C. and Jacob, H. J. (1998). A microsatellite genetic linkage map for zebrafish (*Danio rerio*). *Nat. Genet.* **18,** 338-343.

Knecht, A. K. and Harland, R. M. (1997). Mechanisms of dorsal-ventral patterning in noggin-induced neural tissue. *Development* **124,** 2477-2488.

Knezevic, V., De Santo, R. and Mackem, S. (1998). Continuing organizer function during chick tail development. *Development* **125,** 1791-1801.

Lee, R., Stainier, D., Weinstein, B. and Fishman, M. (1994). Cardiovascular development in the zebrafish. II. Endocardial progenitors are sequestered within the heart field. *Development* **120,** 3361-3366.

Liao, W., Bisgrove, B. W., Sawyer, H., Hug, B., Bell, B., Peters, K., Grunwald, D. J. and Stainier, D. Y. R. (1997). The zebrafish gene *cloche* acts upstream of a *flk-1* homologue to regulate endothelial cell differentiation. *Development* **124,** 381-389.

Lin, J. J., Maeda, R., Ong, R. C., Kim, J., Lee, L. M., Kung, H. F. and Maéno, M. (1997). *XBMP-1B (Xtld)*, a *Xenopus* homolog of dorso-ventral polarity gene in *Drosophila*, modifies tissue phenotypes of ventral explants. *Develop. Growth Differ.* **39,** 43-51.

Maéno, M., Xue, Y., Wood, T. I., Ong, R. C. and Kung, H. (1993). Cloning and expression of cDNA encoding *Xenopus laevis* bone morphogenetic protein-1 during early embryonic development. *Gene* **134,** 257-261.

Marqués, G., Musacchio, M., Shimell, M. J., Wünnenberg-Stapleton, K., Cho, K. W. Y. and O'Connor, M. B. (1997). Production of a DPP Activity Gradient in the Early Drosophila Embryo through the Opposing Actions of the SOG and TLD Proteins. *Cell* **91,** 417-426.

Metz, A., Knöchel, S., Büchler, P., Köster, M. and Knöchel, W. (1998).

Structural and functional analysis of the BMP-4 promoter in early embryos of *Xenopus laevis*. *Mech. Dev.* **74,** 29-39.

Miller-Bertoglio, V., Fisher, S., Sanchez, A., Mullins, M. C. and Halpern, M. E. (1997). Differential regulation of *chordin* expression domains in mutant zebrafish. *Dev. Biol.* **192,** 537-550.

Mullins, M. C. (1998). Holy Tolloido: Tolloid cleaves Sog/Chordin to free DPP/Bmps. *Trends Genet.* **14,** 127-129.

Mullins, M. C. (1999). Embryonic axis formation in the zebrafish. In *Methods in Cell Biology* **59,** 157-176.

Mullins, M. C., Hammerschmidt, M., Kane, D. A., Odenthal, J., Brand, M., van Eeden, F. J. M., Furutani-Seiki, M., Granato, M., Haffter, P., Heisenberg, et al. and Nüsslein-Volhard, C. (1996). Genes establishing dorsoventral pattern formation in the zebrafish embryo: the ventral specifying genes. *Development* **123,** 81-93.

Neave, B., Holder, N. and Patient, R. (1997). A graded response to BMP-4 spatially coordinates patterning of the mesoderm and ectoderm in the zebrafish. *Mech. Dev.* **62,** 183-195.

Nguyen, M., Park, S., Marqués, G. and Arora, K. (1998a). Interpretation of a BMP activity gradient in *Drosophila* embryos depends on synergistic signaling by two type I receptors, SAX and TkV. *Cell* **95,** 495-506.

Nguyen, V. H., Schmid, B., Trout, J., Connors, S. A., Ekker, M. and Mullins, M. C. (1998b). Ventral and Lateral Regions of the Zebrafish Gastrula, Including the Neural Crest Progenitors, are Established by a *bmp2b*/*swirl* Pathway of Genes. *Dev. Biol.* **199,** 93-110.

Nikaido, M., Tada, M., Saji, T. and Ueno, N. (1997). Conservation of BMP signaling in zebrafish mesoderm patterning. *Mech. Dev.* **61,** 75-88.

Pasteels, J. (1943). Proliferations et croissance dans la gastrulation et la formation dela queue des Vertebres. *Arch. Biol.* **54,** 1-51.

Piccolo, S., Agius, E., Lu, B., Goodman, S., Dale, L. and De Robertis, E. M. (1997). Cleavage of Chordin by Xolloid Metalloprotease Suggests a Role for Proteolytic Processing in the Regulation of Spemann Organizer Activity. *Cell* **91,** 407-416.

Rauch, G. J., Granato, M. and Haffter, P. (1997). A polymorphic zebrafish line for genetic mapping using SSLPs on high-percentage agarose gels. *Trends Tech. Tips Online T01208*, http://tto.trends.com/cgibin/tto/pr/pg.

Schulte-Merker, S., Ho, R. K., Herrmann, B. G. and Nüsslein-Volhard, C. (1992). The protein product of the zebrafish homologue of the mouse *T*-gene is expressed in nuclei of the germ ring and the notochord of the early embryo. *Development* **116,** 1021.

Schulte-Merker, S., Lee, K. J., McMahon, A. P. and Hammerschmidt, M. (1997). The zebrafish organizer requires *chordino*. *Nature* **387,** 862-863.

Solnica-Krezel, L., Stemple, D. L., Mountcastle-Shah, E., Rangini, Z., Neuhauss, S. C. F., Malicki, J., Schier, A. F., Stanier, D. Y. R., Zwartkruis, F., Abdelilah, S. and Driever, W. (1996). Mutations affecting cell fates and cellular rearrangements during gastrulation in zebrafish. *Development* **123,** 67-80.

Stöcker, W., Gomis-Rüth, F. X., Bode, W. and Zwilling, R. (1993). Implications of the three-dimensional structure of astacin for the structure and function of the astacin family of zinc-endopeptidases. *Eur. J. Biochem.* **214,** 215-231.

Suzuki, N., Labosky, P. A., Furuta, Y., Hargett, L., Dunn, R., Fogo, A. B., Takahara, K., Peters, D. M. P., Greenspan, D. S. and Hogan, B. L. M. (1996). Failure of ventral body wall closure in mouse embryos lacking procollagen C-proteinase encoded by *BMP1*, a mammalian gene related in *Drosophila tolloid*. *Development* **122,** 3587-3595.

Takahara, K., Brevard, R., Hoffman, G. G., Suzuki, N. and Greenspan, D. S. (1996). Characterization of a novel gene product (mammalian Tolloid-like) with high similarity to mammalian Tolloid/Bone Morphogenic Protein-1. *Genomics* **34,** 157-165.

Takahara, K., Lyons, G. E. and Greenspan, D. S. (1994). Bone Morphogenic Protein-1 and a Mammalian Tolloid Homologue (mTld) Are Encoded by Alternatively Spliced Transcripts Which Are Differentially Expressed in Some Tissues. *J. Biol. Chem.* **269,** 32572-32578.

Thompson, M. A., Ransom, D. G., Pratt, S. J., MacLennan, H., Kieran, M. W., Detrich, H. W., Vail, B., Huber, T. L., Paw, B., Brownlie, A. J., et al. and Zon, L. I. (1998). The *cloche* and *spadetail* genes differentially affect hematopoiesis and vasculogenesis. *Dev. Biol.* **197,** 248-269.

Thomsen, G. H. (1997). Antagonism within and around the organizer: BMP inhibitors in vertebrate body patterning. *Trends Genet.* **13,** 209-211.

Tucker, A. S. and Slack, J. M. W. (1995). The *Xenopus laevis* tail-forming region. *Development* **121,** 249-262.

Weinberg, E. S., Allende, M. L., Kelly, C. L., Abdelhamid, A., Murakami, T., Andermann, P., Doerre, G., Grunwald, D. J. and Riggleman, B. (1996). Developmental regulation of zebrafish *MyoD* in wild-type, *no tail*, and *spadetail* embryos. *Development* **122,** 271-280.

Westerfield, M. (1995). *The Zebrafish Book: A Guide for the Laboratory Use of Zebrafish (*Danio rerio*).* University of Oregon Press.

Wilson, P. A., Lagna, G., Suzuki, A. and Hemmati-Brivanlou, A. (1997). Concentration-dependent patterning of the *Xenopus* ectoderm by BMP4 and its signal transducer Smad1. *Development* **124,** 3177-3184.

Woo, K. and Fraser, S. E. (1998). Specification of the Hindbrain Fate in the Zebrafish. *Dev. Biol.* **197,** 283-296.